



Green one-pot synthesis of 2*H*-indazolo[2,1-*b*]phthalazine-triones: a comparative study of heterogeneous solid acid catalysts with magnetic core

Mahdia Hamidinasab^{1,2} · Akbar Mobinikhaledi^{1,2}

Received: 3 August 2018 / Accepted: 11 January 2019
© Iranian Chemical Society 2019

Abstract

The catalytic activity of four heterogeneous solid acid catalysts with magnetic core and sulfonic acid groups is evaluated and compared using one-pot three component synthesis of phthalazine-trione derivatives under solvent-free condition. The NiFe₂O₄ particles were selected as magnetic core, due to their enhanced chemical and magnetic stability. Furthermore, the desired products were obtained in excellent yields at short reaction times and environmentally friendly condition using the novel and reusable sulfonic acid grafted onto TiO₂-coated nickel ferrite nanoparticles. This protocol avoids the use of expensive catalysts, toxic solvents and harsh reaction conditions.

Keywords Phthalazine-trione · Multicomponent reaction · Magnetic nanoparticles · Heterogeneous catalysis · Hybrid materials · Green condition

Introduction

Recently, considerable attention has been focused on synthesis of phthalazine derivatives [1–4] as they possess different pharmaceutical and biological activities such as antimicrobial [5], vasorelaxant [6], antifungal [7], anticancer [8] and anti-inflammatory activities [9]. Several methods have been reported for synthesis of phthalazine derivatives. However, the traditional method of synthesis of these valuable compounds plays an important role in modern synthetic methods.

Multicomponent reactions (MCRs) are important reactions in modern organic synthesis in which three or more different compounds react to give a single product (so-called domino). These reactions are applicable for synthesis of different compounds, usually in a one-pot procedure and all of the reagents are incorporated into the final product and cause short reaction time and simplify purification. As a result,

MCRs can be used as powerful approaches for synthesizing of these vital and pharmaceutical compounds.

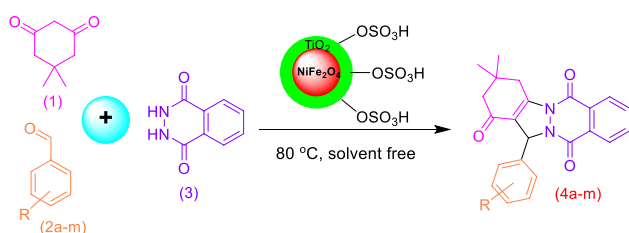
Nanocatalysis is a rapidly growing field in green chemistry, which involves the use of nanomaterials as catalysts for various chemical reactions. By altering the size, morphology, composition and chemical stability of nanomaterials, a novel catalyst with modified properties can be achieved. Nanocatalysts have both properties of homogeneous and heterogeneous catalysts; therefore, they are more efficient than normal homogeneous and heterogeneous catalysts for chemical reactions [10, 11]. In recent years, the use of magnetic nanoparticles (MNPs) has found special interest due to their super magnetic behaviors, easy separation from the reaction media, large surface area, low toxicity, good stability and possible functionalization [12–16].

In view of these reports and also due to development of green procedures for synthesis of valuable heterocyclic compounds, herein we wish to report an environmentally benign protocol for synthesis of some phthalazine-trione derivatives via three-component condensation of phthalhydrazide, dimedone and aldehydes in the presence of sulfonic acid grafted TiO₂-coated nickel–ferrite nanoparticles under solvent-free condition (Scheme 1).

✉ Mahdia Hamidinasab
mahdiahamidinasab@yahoo.com

¹ Department of Chemistry, Faculty of Science, Arak University, Arak 38156-88138, Iran

² Institute of Nanosciences and Nanotechnology, Arak University, Arak 38156-88138, Iran



Scheme 1 The synthetic pathway of *2H*-indazolo[2,1-*b*]phthalazine-triones via three-component condensation reaction using functionalized magnetic nickel ferrite nanoparticles

Experimental

Chemicals and apparatus

All chemicals were purchased from Merck or Fluka chemical companies and used without further purification. Melting points were measured using capillary tubes on an electrothermal digital apparatus and all products were identified by comparison of their melting points and spectral data with those reported in the literature. Thin layer chromatography (TLC) was performed on UV active aluminum backed plates of silica gel. FT-IR spectra were recorded on a Unicom Galaxy Series FT-IR 5000 spectrophotometer in the region of 400–4000 cm^{-1} using pressed KBr discs. The ^1H and ^{13}C -NMR spectra were recorded on a Bruker Avance spectrometer operating at 300 and 75 MHz for ^1H and ^{13}C -NMR, respectively. Tetramethylsilane (TMS) was used as an internal standard. X-ray diffraction (XRD) was performed on Philips PW1730 Cu-K α radiation of wavelength 1.54 Å. Thermal gravimetric analysis (TGA) and differential thermal gravimetric (DTG) data for $\text{NiFe}_2\text{O}_4@ \text{TiO}_2\text{-SO}_3\text{H}$ were recorded on a Mettler TGA/STTA351 System under an N_2 atmosphere at a heating rate of 10 $^\circ\text{C min}^{-1}$. The scanning electron microscopy measurement was carried out on a tescan mira II field emission-scanning electron magnetization (FE-SEM) and hysteresis loop were measured at room temperature using a Vibrating Sample Magnetometer (Model 7300 VSM system, Lake Shore Cryotronic, Inc., Westerville, OH, USA).

Preparation of nickel ferrite nanoparticles

NiFe_2O_4 nanoparticles were synthesized by co-precipitation method [17]. Aqueous solutions of Nickel chloride and ferric chloride (1:2) were prepared in de-ionized water (25 mL) and the NaOH solution (3 M) was slowly added and stirred continuously using a stirrer to reach the pH 12. The mixture was heated at 80 $^\circ\text{C}$ for 4 h. The result was

filtered and washed three times with deionized water and ethanol and dried at 60 $^\circ\text{C}$. The dried powder was annealed at 400 $^\circ\text{C}$ for 3 h.

Preparation of titania-coated nickel ferrite magnetic nanoparticles

0.5 g of NiFe_2O_4 MNPs was sonicated in 60 mL ethanol-acetonitrile (2:1) for 1 h. Then aqueous ammonia 25% (1 mL) and tetraethyl orthotitanate (TEOT, 0.5 mL) were added to this suspension. The mixture was stirred at room temperature for 24 h. The titania-modified nanoparticles were isolated by external magnet and rinsed with ethanol and distilled water three times and dried at 80 $^\circ\text{C}$ [18].

Preparation of the nano- $\text{NiFe}_2\text{O}_4@ \text{TiO}_2\text{-SO}_3\text{H}$

0.5 g of $\text{NiFe}_2\text{O}_4@ \text{TiO}_2$ MNPs was poured into a flask. Then a solution of 0.3 mL of chlorosulfonic acid in 10 mL CH_2Cl_2 was added dropwise over a period of 30 min at room temperature (Caution: a highly corrosive and water absorbent. Be careful when using this liquid. Protective gloves, protective clothing and eye and face protection equipment's are needed). A powder of $\text{NiFe}_2\text{O}_4@ \text{TiO}_2$ MNP-supported sulfonic acid was obtained. The resulting nanoparticles were then washed with ethanol and distilled water three times and dried at 70 $^\circ\text{C}$.

General procedure for synthesis of *2H*-indazolo[2,1-*b*]phthalazine-trione derivatives

A mixture of dimedone (0.14 g, 1 mmol), phthalhydrazide (0.16 g, 1 mmol), aromatic aldehyde (1 mmol), and nano-catalyst (0.03 g) was heated at 80 $^\circ\text{C}$ for 10 min (TLC). After cooling, the reaction mixture was poured in 10 mL of DMF and the catalyst was separated easily by an external magnet. The saturated sodium chloride solution was then added to precipitate the pure product.

Selected spectroscopic and physical data for products

3,4-Dihydro-3,3-dimethyl-13-phenyl-2*H*-indazolo[2,1-*b*]phthalazine-1,6,11(13*H*)-trione (4a)

Yellow powder, M.P.: 201–203 $^\circ\text{C}$; IR (KBr) (ν_{max} , cm^{-1}): 3018, 1668, 1601, 1556, 1493, 1294; δ_{H} (300 MHz, $\text{DMSO-}d_6$) 1.09 (6H, s, 2Me), 2.24 (2H, s, CH_2C), 3.18 (2H, s, CH_2CO), 6.26 (1H, s, CHN), 7.28–8.24 (9H, m, Ar-H).

3,4-Dihydro-3,3-dimethyl-13-(3-nitrophenyl)-2H-indazolo[2,1-b]phthalazine-1,6,11(13H)-trione (4b)

Yellow powder, M.P.: 265–267 °C; IR (KBr) (ν_{\max} , cm^{-1}): 3119, 1660, 1626, 1529, 1361, 1313; δ_{H} (300 MHz, DMSO- d_6) 1.11 and 1.13 (6H, s, 2Me), 2.26 (2H, s, CH_2C), 3.22 (2H, m, CH_2CO), 6.48 (1H, s, CH), 7.59–8.37 (8H, m, Ar-H); δ_{C} (75 MHz, DMSO- d_6) 28.2, 28.5, 34.7, 37.7, 50.6, 64.1, 116.6, 122.9, 123.5, 127.2, 127.9, 128.8, 129.7, 130.2, 134.7, 134.9, 140.1, 148.1, 152.5, 154.4, 155.9, 192.3.

Results and discussion

Preparation and characterization of novel MNPs catalyst

In recent years, many studies have reported the use of magnetite (Fe_3O_4) as magnetic nanoparticles. In the present work, nickel ferrite (NiFe_2O_4) nanoparticles were used as a catalyst instead of magnetite nanoparticles. The preparation of NiFe_2O_4 is easier than that of Fe_3O_4 as it is not sensitive to oxygen and the use of inert atmosphere such as N_2 during the reaction is not needed. Another important advantage of NiFe_2O_4 was proved by magnetic hysteresis loops. For comparison of these two magnetic nanoparticles (Fe_3O_4 and NiFe_2O_4) we have synthesized them under the same conditions. The magnetic properties of nanoparticles were characterized using a vibrating sample magnetometer (VSM). In Fig. 1, the typical room temperature magnetization curves of NiFe_2O_4 and Fe_3O_4 nanoparticles are shown. The saturation magnetization (M_s) of these nanoparticles changes from 35.1 emu g^{-1} for NiFe_2O_4 to 32.2 emu g^{-1} for Fe_3O_4 core.

For the coating of nanoparticles, TEOT and TEOS were used as coating reagents and the results were compared. TEOT and TEOS are not significantly different in terms of

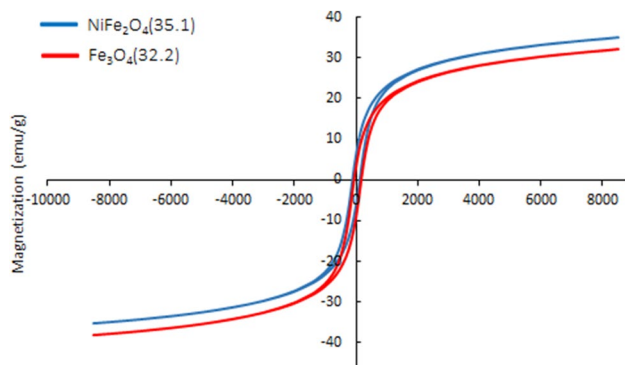


Fig. 1 The comparison of magnetic hysteresis loops of NiFe_2O_4 and Fe_3O_4 nanoparticles

toxicity, albeit it can be said that TEOT is a little bit safer than TEOS. The electronegativity difference ($\Delta\chi$) of Ti–O and Si–O bonds is 2.2 and 1.7, respectively. Therefore, we think that the reactivity of TEOT, with hydroxyl groups on nanoparticles surfaces, is higher than that of TEOS. The vibrating sample magnetometer (VSM) technique was used to prove this hypothesis (Fig. 2). The M_s of $\text{NiFe}_2\text{O}_4@ \text{TiO}_2$ was 27.1 while the M_s of $\text{NiFe}_2\text{O}_4@ \text{SiO}_2$ was 29.6, which represents the higher magnetic loss for titania coating (8 emu g^{-1}) than silica (5.5 emu g^{-1}). The results confirm that TEOT coated the nanoparticles with higher thickness.

For further investigation, different amounts of TEOT (5, 10 and 15 mmol) were reacted with NiFe_2O_4 nanoparticle surfaces. Then, the magnetic properties of nanoparticles were characterized using VSM (Fig. 3). The best result was for 10 mmol of TEOT and there was no significant change for 15 mmol.

Finally, Sulfonic acid-grafted titania-coated nickel ferrite nanoparticles were prepared using the procedure presented in Scheme 2. In summary, NiFe_2O_4 nanoparticles were easily

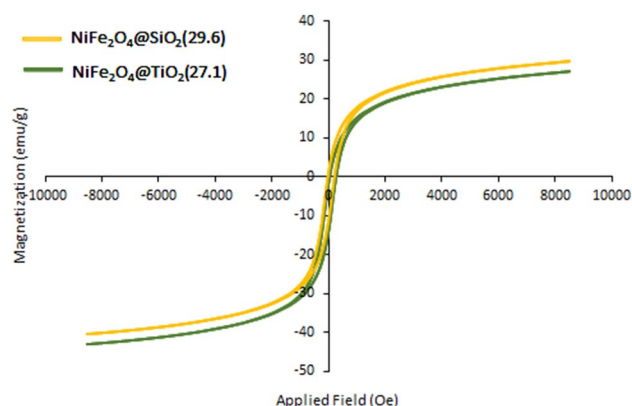


Fig. 2 The comparison of magnetic hysteresis loops of $\text{NiFe}_2\text{O}_4@ \text{TiO}_2$ and $\text{NiFe}_2\text{O}_4@ \text{SiO}_2$ nanoparticles

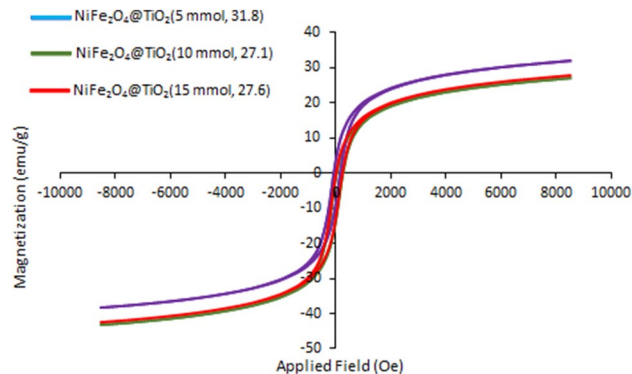
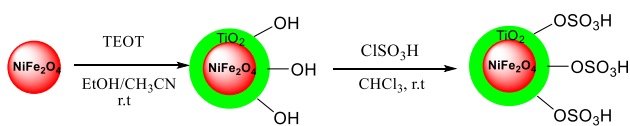


Fig. 3 The comparison of magnetic hysteresis loops of $\text{NiFe}_2\text{O}_4@ \text{TiO}_2$ nanoparticles with different shell thickness



Scheme 2 Preparation of nano- $\text{NiFe}_2\text{O}_4@ \text{TiO}_2\text{-SO}_3\text{H}$

prepared via the chemical co-precipitation of Ni^{2+} and Fe^{3+} ions in basic solution [17]. The prepared NiFe_2O_4 nanoparticles were subsequently coated with titania through the easy protocol [11, 19–21]. The free OH groups on TiO_2 -coated nickel ferrite nanoparticles were reacted with chlorosulfonic acid to give the sulfonic acid-grafted TiO_2 -coated nickel ferrite nanoparticles ($\text{NiFe}_2\text{O}_4@ \text{TiO}_2\text{-SO}_3\text{H}$). For comparison study of catalytic activity, the nano- $\text{NiFe}_2\text{O}_4@ \text{SiO}_2\text{-SO}_3\text{H}$ [22], nano- $\text{Fe}_3\text{O}_4@ \text{SiO}_2\text{-SO}_3\text{H}$ [23] and nano- $\text{Fe}_3\text{O}_4@ \text{TiO}_2\text{-SO}_3\text{H}$ [11] were prepared according to the reported procedures.

The prepared acidic magnetic nanoparticles were characterized by the various standard techniques, including Fourier transform infrared (FT-IR) spectroscopy, field emission scanning electron microscopy (FE-SEM), energy dispersive X-ray spectroscopy (EDS), vibrating sample magnetometer (VSM), X-ray diffraction (XRD) and thermogravimetric analysis (TGA).

The FT-IR Spectra of NiFe_2O_4 MNPs, $\text{NiFe}_2\text{O}_4@ \text{TiO}_2$ core-shell MNPs, $\text{NiFe}_2\text{O}_4@ \text{TiO}_2\text{-SO}_3\text{H}$, are presented in Fig. 4. In curve (a), the spectrum of NiFe_2O_4 nanoparticles shows strong absorption bands around 401 cm^{-1} and 601 cm^{-1} , corresponding to stretching vibration of metal-O at octahedral site and metal-O of tetrahedral site [24]. The low-frequency absorption band at 1400 cm^{-1} in curve (b) is assigned to the stretching vibration of Ti-O-Ti. The broad peaks in the range of $3000\text{--}3600\text{ cm}^{-1}$ and the weak peak at 1631 cm^{-1} are due to the O-H stretching vibration mode

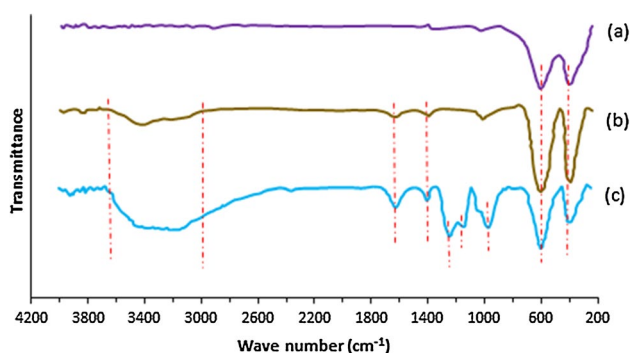


Fig. 4 The FT-IR spectra of (a) nano- NiFe_2O_4 (b) nano- $\text{NiFe}_2\text{O}_4@ \text{TiO}_2$ and (c) nano- $\text{NiFe}_2\text{O}_4@ \text{TiO}_2\text{-SO}_3\text{H}$ catalyst

(Ti-O) and twisting vibration mode of H-O-H adsorbed in the titania shell, respectively. In curve (c) we can find the

O=S=O asymmetric and symmetric stretching vibration and S-O stretching vibration of sulfonic groups, respectively, at 1242 cm^{-1} , 1145 cm^{-1} , 974 cm^{-1} [11, 25], respectively.

The morphology of $\text{NiFe}_2\text{O}_4@ \text{TiO}_2\text{-SO}_3\text{H}$ was characterized by FE-SEM. Figure 5 indicates that these modified titania-coated MNPs are almost spherical with regular shape and the average particle size is about 37.1 nm, as indicated by the size histogram in Fig. 6B. Figure 6A shows the X-ray diffraction patterns of the synthesized NiFe_2O_4 nanoparticle and modified nano- $\text{NiFe}_2\text{O}_4@ \text{TiO}_2\text{-SO}_3\text{H}$ particles. Several peaks appeared at values of (111), (220), (311), (222), (400), (422), (511), (440) and (533) indicating a cubic crystal system for NiFe_2O_4 nanoparticles (Fig. 6A curve (a)), [26, 27], which conforms with JCPDS file (no. 44-1485) standard [24]. The peak at $2\theta = 26.6^\circ$ confirms the formation of TiO_2 shell (Fig. 6A curve (a)) [27].

The average size of the crystallites was calculated by applying Scherer's equation: $D = 0.9\lambda / \beta \cos \theta$, where h is the diffraction angle, λ is the wavelength of the incident X-rays, β is full width at half maximum height in radians, θ is the Bragg diffraction angle and D is the average diameter in Å. The peak at $2\theta = 35.7^\circ$ is selected to calculate the crystallite size, according to the result calculated by Scherer's equation; it is found that the diameter of nano- $\text{NiFe}_2\text{O}_4@ \text{TiO}_2\text{-SO}_3\text{H}$ particles is about 43.1 nm, which is in the range determined using size histogram analysis (Fig. 6B).

The energy-dispersive X-ray spectroscopy (EDS) of $\text{NiFe}_2\text{O}_4@ \text{TiO}_2\text{-SO}_3\text{H}$ is shown in Fig. 7. The presence of Fe, Ni, O, S and Ti atoms was observed in the EDX spectrum. The presence of Ti, O and Ni signals confirms the existence of titania shell on the nickel ferrite nanoparticles. Furthermore, the EDX maps of $\text{NiFe}_2\text{O}_4@ \text{TiO}_2\text{-SO}_3\text{H}$ nanoparticles are presented in Fig. 8. According to the results, there is a good dispersion of Fe, Ni, O, S and Ti elements on the surface of $\text{NiFe}_2\text{O}_4@ \text{TiO}_2\text{-SO}_3\text{H}$ nanoparticles.

The stability of the $\text{NiFe}_2\text{O}_4@ \text{TiO}_2\text{-SO}_3\text{H}$ catalyst was determined by thermogravimetric analysis (TGA) and derivative thermogravimetry (DTG) (Fig. 9). The TGA curve of magnetic catalyst shows an initial 2% weight loss from r.t to about 250°C , which is due to the removal of physically adsorbed solvent and surface hydroxyl groups (Fig. 9). The major weight loss beyond 200°C to nearly 650°C is attributed to the decomposition of the sulfonic acid groups in the nanocomposite. Therefore, the catalyst is reasonably stable up to 250°C and it is safe to use under thermal reaction condition. The grafted sulfonic acid content on the $\text{NiFe}_2\text{O}_4@ \text{TiO}_2$ is approximately 8 wt%. Moreover, the DTG curve indicates that the deformation of the inorganic structure mainly occurred at 710°C . Therefore, the $\text{NiFe}_2\text{O}_4@ \text{TiO}_2\text{-SO}_3\text{H}$ is stable around or below 300°C (Fig. 9).

The magnetic properties of nanoparticles were characterized using a vibrating sample magnetometer (VSM). Figure 10 shows the typical room temperature magnetization

Fig. 5 The FE-SEM image of $\text{NiFe}_2\text{O}_4@ \text{TiO}_2\text{-SO}_3\text{H}$ nanoparticles (200, 500 nm)

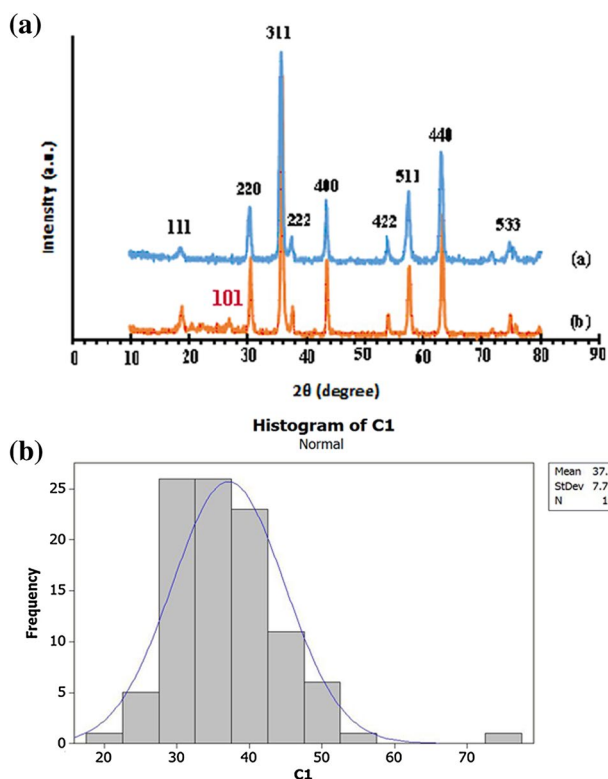
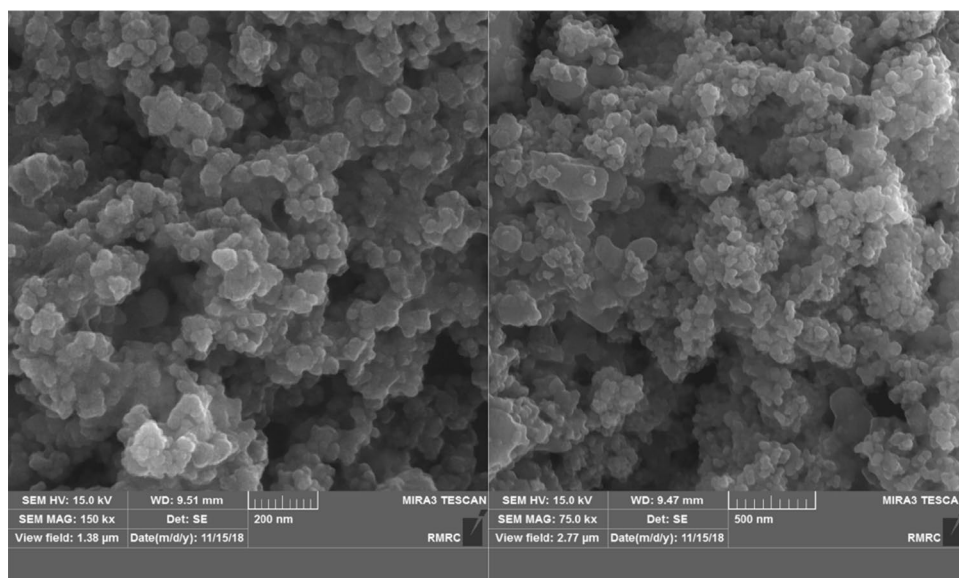


Fig. 6 A The XRD patterns of (a) NiFe_2O_4 nanoparticle and (b) nano- $\text{NiFe}_2\text{O}_4@ \text{TiO}_2\text{-SO}_3\text{H}$. B The particle size distribution histogram of spherical acidic modified nano- $\text{NiFe}_2\text{O}_4@ \text{TiO}_2\text{-SO}_3\text{H}$

curves of NiFe_2O_4 MNPs (Fig. 10, curve a), and $\text{NiFe}_2\text{O}_4@ \text{TiO}_2\text{-SO}_3\text{H}$ (Fig. 10, curve b). The hysteresis curve allows determination of the coercivity (H_c), remanent magnetization (M_r) and saturation magnetization (M_s). The magnetization of sample could be completely saturated at high fields of

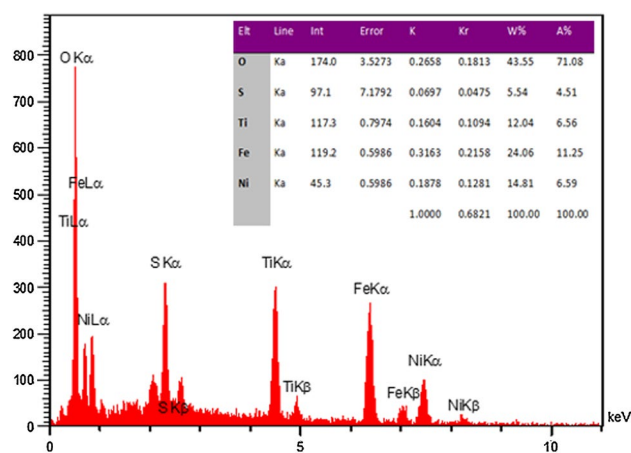


Fig. 7 The EDS spectrum of modified nano- $\text{NiFe}_2\text{O}_4@ \text{TiO}_2\text{-SO}_3\text{H}$ particles

up to ± 8000.0 Oe and, M_s of samples changes from 35.1 to 21.1 emu g^{-1} due to the formation of a titania shell and inorganic layer around the NiFe_2O_4 core. The hysteresis loops show the superparamagnetic behaviour of the NiFe_2O_4 and $\text{NiFe}_2\text{O}_4@ \text{TiO}_2\text{-SO}_3\text{H}$ particles in which M_r and H_c are close to zero ($M_r = 119$ and 154 emu g^{-1} and $H_c = 4.1$ and 6.1 Oe, respectively) [28].

Acidity of $\text{NiFe}_2\text{O}_4@ \text{TiO}_2\text{-SO}_3\text{H}$

The concentration of grafted sulfonic acid on the $\text{NiFe}_2\text{O}_4@ \text{TiO}_2\text{-SO}_3\text{H}$, $\text{NiFe}_2\text{O}_4@ \text{SiO}_2\text{-SO}_3\text{H}$, $\text{Fe}_3\text{O}_4@ \text{TiO}_2\text{-SO}_3\text{H}$ and $\text{Fe}_3\text{O}_4@ \text{SiO}_2\text{-SO}_3\text{H}$ nanomaterials was determined via a back titration with HCl (0.01 N). A solution of KOH (2 mL, 0.01 N) was added to 0.02 g of the magnetic nanoparticles and the mixture was stirred at room temperature for 30 min. The catalyst

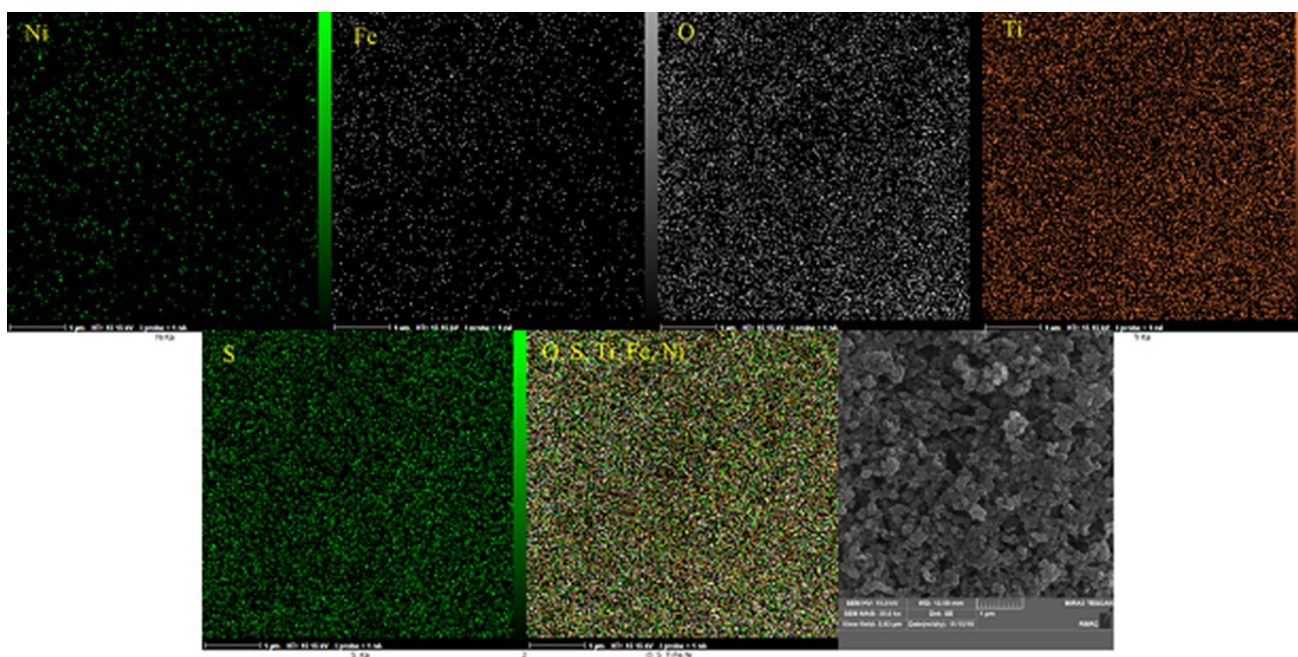


Fig. 8 The FE-SEM image and EDX maps of NiFe₂O₄@TiO₂-SO₃H nanoparticles

was magnetically separated and washed with deionized water. The excess amount of KOH was titrated with HCl (0.01 N) in the presence of phenolphthalein as an indicator. The results revealed that the NiFe₂O₄@TiO₂-SO₃H, NiFe₂O₄@SiO₂-SO₃H, Fe₃O₄@TiO₂-SO₃H and Fe₃O₄@SiO₂-SO₃H have 2.9, 2.3, 2.8 and 2.1 mmol g⁻¹ acid content, respectively. These results confirm the greater porosity of silica layer.

Synthesis of 2*H*-indazolo[2,1-*b*]phthalazine-triones derivatives

After the characterization of the NiFe₂O₄@TiO₂-SO₃H nanoparticles, its role as a catalyst was evaluated for synthesis of 2*H*-indazolo[2,1-*b*]phthalazine-triones **4a–m** (Scheme 1). For optimization of reaction conditions, a one-pot three-component condensation reaction of dimedone **1** (1 mmol), benzaldehyde **2a** (1 mmol) and phthalhydrazide **3** (1 mmol) was used as a model reaction. At first, to investigate the efficiency of the catalyst the model reaction was carried out in several solvents such as CH₃CN, EtOH, THF, toluene and H₂O under reflux as well as under solvent-free conditions (Table 1). As shown in Table 1, it was found that conventional heating at 80 °C under solvent-free conditions is more efficient than using organic solvents, with respect to reaction time and yield of the desired product (Table 1, entry 9). The effect of catalyst amount on reaction yield was studied using various amounts of NiFe₂O₄@TiO₂-SO₃H. The results displayed that 30 mg of the nanocatalyst

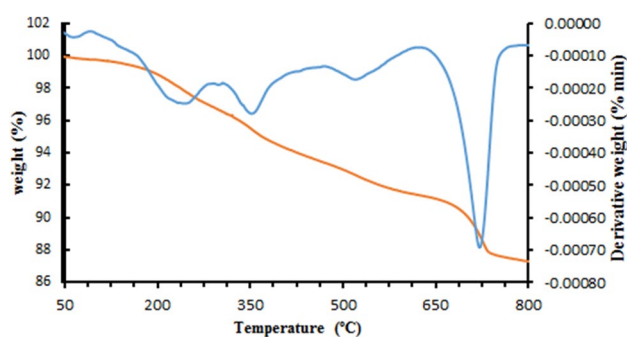


Fig. 9 TG-DTG curves of NiFe₂O₄@TiO₂-SO₃H nanoparticles

is sufficient to complete the reaction after 5 min in 92% (Table 1, entry 10). To define the role of NiFe₂O₄@TiO₂-SO₃H as a catalyst for the preparation of 2*H*-indazolo[2,1-*b*]phthalazine-trione derivatives, the model reaction was carried out with NiFe₂O₄, NiFe₂O₄@TiO₂-SO₃H and without the catalyst (Table 1, entries 12–14). With respect to yield of product and reaction time, the best results are attained using NiFe₂O₄@TiO₂-SO₃H as the catalyst. To compare the catalytic activity, the same reactions were carried out in the presence of as-prepared solid acids: nano-Fe₃O₄@TiO₂-SO₃H, nano-NiFe₂O₄@SiO₂-SO₃H and nano-Fe₃O₄@SiO₂-SO₃H. As presented in Table 1 (entry 10, 15, 17 and 18), the yield and activity of them are almost the same. The magnetic core of NiFe₂O₄@TiO₂ particles is more stable than others and so is the best choice for this reaction [29, 30].

Table 1 Optimization of reaction conditions for synthesis of 2*H*-indazolo[2,1-*b*]phthalazine-trione

Entry	Catalyst (mg)	Solvent	Temp. (°C)	Time	Yield (%) ^a
1	NiFe ₂ O ₄ @TiO ₂ -SO ₃ H (10)	CH ₃ CN	Reflux	6 h	75
2	NiFe ₂ O ₄ @TiO ₂ -SO ₃ H (10)	EtOH	Reflux	3 h	86
3	NiFe ₂ O ₄ @TiO ₂ -SO ₃ H (10)	THF	Reflux	3.5 h	78
4	NiFe ₂ O ₄ @TiO ₂ -SO ₃ H (10)	H ₂ O	Reflux	4 h	71
5	NiFe ₂ O ₄ @TiO ₂ -SO ₃ H (10)	CHCl ₃	Reflux	4 h	81
6	NiFe ₂ O ₄ @TiO ₂ -SO ₃ H (10)	Toluene	Reflux	8 h	73
7	NiFe ₂ O ₄ @TiO ₂ -SO ₃ H (10)	Solvent-free	rt	10 h	39
8	NiFe ₂ O ₄ @TiO ₂ -SO ₃ H (10)	Solvent-free	50	3 h	89
9	NiFe ₂ O ₄ @TiO ₂ -SO ₃ H (10)	Solvent-free	80	5 min	85
10	NiFe₂O₄@TiO₂-SO₃H (30)	Solvent-free	80	5 min	92
11	NiFe ₂ O ₄ @TiO ₂ -SO ₃ H (50)	Solvent-free	80	5 min	92
12	–	Solvent-free	80	1 h	51
13	NiFe ₂ O ₄ (30)	Solvent-free	80	30 min	78
14	NiFe ₂ O ₄ @TiO ₂ (30)	Solvent-free	80	30 min	67
15	NiFe₂O₄@SiO₂-SO₃H (30)	Solvent-free	80	5 min	93
16	Fe ₃ O ₄ (30)	Solvent-free	80	45 min	59
17	Fe₃O₄@SiO₂-SO₃H (30)	Solvent-free	80	5 min	91
18	Fe₃O₄@TiO₂-SO₃H (30)	Solvent-free	80	5 min	90

Reaction conditions: dimedone (1 mmol), phthalhydrazide (1 mmol), benzaldehyde (1 mmol) and nanocatalyst

Bold rows are optimum conditions

^aIsolated yield

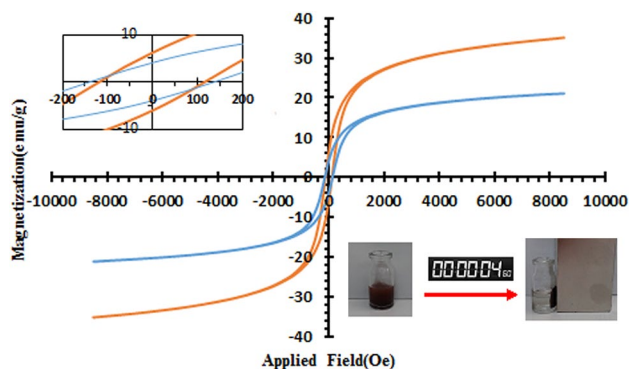


Fig. 10 Magnetic hysteresis loops of (a) NiFe₂O₄ MNPs and (b) NiFe₂O₄@TiO₂-SO₃H nanoparticles

As shown in Table 2, various aldehydes (**2a–m**) reacted with phthalhydrazide (**1**) and dimedone (**2**) to give the corresponding 2*H*-indazolo[2,1-*b*]phthalazine-triones (**4a–m**) with good to excellent yields under optimized conditions. Arylaldehydes with electron-donating or electron-withdrawing groups could lead to the favourite products. Aliphatic aldehydes were also used, but did not afford desired products.

To demonstrate the applicability of our catalyst, the condensation reaction of benzaldehyde, dimedone and phthalhydrazide under optimized conditions for synthesis of 2*H*-indazolo[2,1-*b*]phthalazine-trione in the presence of NiFe₂O₄@TiO₂-SO₃H nanoparticles was carried out and

the results were compared with other used catalysts in this reaction (Table 3). As can be seen, the catalytic system reported in this paper has benefits in terms of simple condition, reaction time and yield.

The formation of products **4a–m** can be rationalized by initial formation of intermediate **1'** by standard Knoevenagel condensation of dimedone **1** and aldehyde **2** in the presence of acidic nanocatalyst. Then, the subsequent Michael-type addition of the phthalhydrazide **3** to the intermediate **1'**, produces intermediate **2'** that followed by cyclization and tautomerization and affords the corresponding product **4** (Scheme 3).

Catalyst recovery and reusability

The recovery and recyclability of the catalyst are important features for industrial and commercial applications. Thus reusability of the nano-NiFe₂O₄@TiO₂-SO₃H particles was investigated by three-component reaction of dimedone (1 mmol), phthalhydrazide (1 mmol) and benzaldehyde (1 mmol) in the presence of catalyst (0.03 g).

After completion of the reaction, the nanocatalyst was easily separated using an external magnet, washed with EtOH, double distilled water and then dried. The catalyst could be used at least six times without significant loss of activity as seen in Fig. 11. The FT-IR spectrum of the catalyst after six runs confirmed its stability (Fig. 11).

Table 2 The synthesis of 2*H*-indazolo[2,1-*b*]phthalazine-triones using NiFe₂O₄@TiO₂-SO₃H nanoparticles as a catalyst

Entry	Aldehyde	Product	Time (min)	Yield (%)	M.p (°C) [lit]	Refs.
1	Benzaldehyde	4a	5	92	205 [31]	
2	3-Nitrobenzaldehyde	4b	10	95	268 [31]	
3	4-Chlorobenzaldehyde	4c	10	89	260 [31]	
4	4-Methoxybenzaldehyde	4d	30	88	257 [32]	
5	4-Hydroxybenzaldehyde	4e	20	89	266 [32]	
6	4-Bromobenzaldehyde	4f	10	91	262 [31]	
7	2-Chlorobenzaldehyde	4g	10	90	265 [31]	
8	4-Fluorobenzaldehyde	4h	10	93	215 [31]	
9	4-Nitrobenzaldehyde	4i	5	94	226 [31]	
10	2,4-Dichlorobenzaldehyde	4j	10	92	207 [33]	
11	2-Hydroxybenzaldehyde	4 k	20	91	185 [34]	
12	3,4-Dimethoxybenzaldehyde	4l	35	87	206 [32]	
13	4-(Dimethylamino)benzaldehyde	4m	20	88	257 [32]	

Reaction conditions: dimedone (1 mmol), phthalhydrazide (1 mmol), aldehyde (1 mmol) and nanocatalyst (0.03 mmol)

Bold rows are optimum conditions

^aIsolated yield

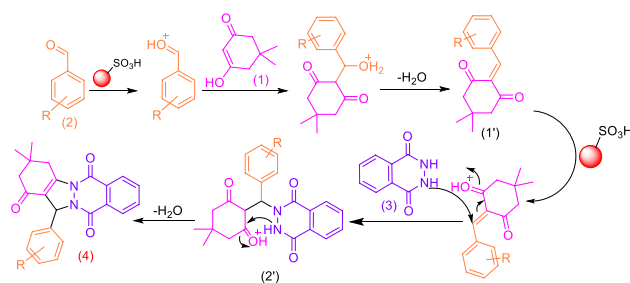
Table 3 Comparison of MNPs-titania sulfuric acid with other catalysts described in the literature for synthesis of 2*H*-indazolo[2,1-*b*]phthalazine-trione via three-component reaction

Entry	Catalyst	Condition	Time	Yield ^a (%)	Refs.
1	H ₃ PW ₁₂ O ₄₀	Ionic liquid	30 min	92	[35]
2	WO ₃ /ZrO ₂	CH ₃ CN (80 °C)	5 h	85	[33]
3	CAN	PEG400 (50 °C)	2 h	94	[34]
4	PSA	Solvent-free (100 °C)	10 min	91	[36]
5	p-TSA	Solvent-free (80 °C)	10 min	86	[31]
6	H ₂ SO ₄	H ₂ O-EtOH (reflux)	30 min	88	[32]
7	H ₂ SO ₄	[bmim]BF ₄	35 min	91	[32]
8	Silica-SO ₃ H	Solvent-free (100 °C)	8 min	87	[37]
9	SO ₃ H-FMSM	Solvent-free (100 °C)	20 min	93	[38]
10	MNPs-Titania sulfuric acid	Solvent-free (80 °C)	5 min	92	Present work

Reaction conditions: dimedone (1 mmol), phthalhydrazide (1 mmol), benzaldehyde (1 mmol) and catalyst

Conclusion

In summary, the catalytic activity of four heterogeneous solid acid catalysts with magnetic core was compared using one-pot three component synthesis of phthalazine-trione derivatives under solvent-free condition. Finally, the nano-NiFe₂O₄@TiO₂-SO₃H as a novel and retrievable catalyst with high stability was used for synthesis of several phthalazine-triones. Mild reaction conditions, operational simplicity, enhanced rates, high isolated yields of pure products, good thermal and chemical stability of nanocatalyst are main and remarkable advantages of described protocol.



Scheme 3 Schematic plausible mechanism for synthesis of 2*H*-indazolo[2,1-*b*]phthalazine-triones in the presence of MNPs-titania sulfuric acid via three-component condensation reaction

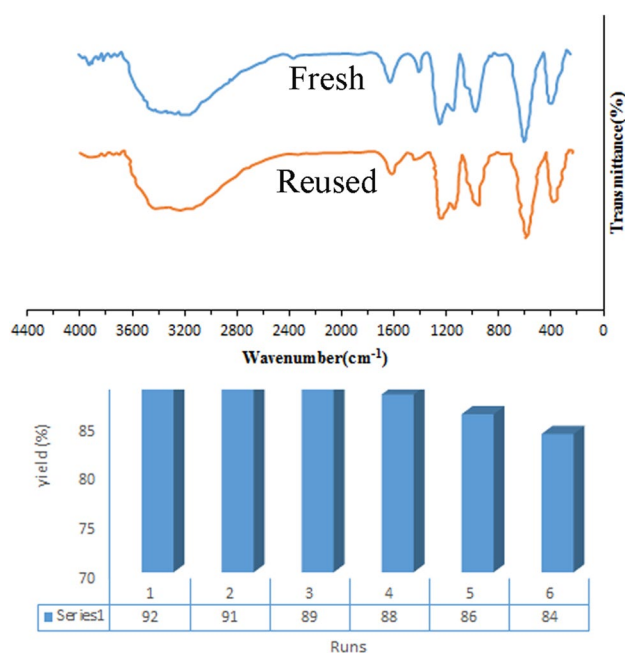


Fig. 11 The FT-IR spectra of the fresh and the six-times reused catalyst and recyclability spectrum of MNPs-silica sulfuric acid for synthesis of 2*H*-indazolo[2,1-*b*]phthalazine-trione

Acknowledgements This work was supported by the research council of Arak University (Grant no. 9312432101). The authors acknowledge wholeheartedly the help received from colleague Dr. Mohammad Ali Bodaghifard from “Department of Chemistry”. There are no conflicts of interest to disclose.

References

- L.-P. Liu, J.-M. Lu, M. Shi, *Org. Lett.* **9**, 1303 (2007)
- R. Ghahremanzadeh, G.I. Shakibaei, A. Bazgir, *Synlett* **2008**, 1129 (2008)
- R. Ghahremanzadeh, S. Ahadi, M. Sayyafi, A. Bazgir, *Tetrahedron Lett.* **49**, 4479 (2008)
- M.R. Nabid, S.J.T. Rezaei, R. Ghahremanzadeh, A. Bazgir, *Ultrason. Sonochem.* **17**, 159 (2010)
- S.S. El-Sakka, A. Soliman, A. Imam, *Afinidad* **66**, 167 (2009)
- N. Watanabe, Y. Kabasawa, Y. Takase, M. Matsukura, K. Miyazaki, H. Ishihara, K. Kodama, H. Adachi, *J. Med. Chem.* **41**, 3367 (1998)
- C.-K. Ryu, R.-E. Park, M.-Y. Ma, J.-H. Nho, *Bioorg. Med. Chem. Lett.* **17**, 2577 (2007)
- J. Li, Y.-F. Zhao, X.-Y. Yuan, J.-X. Xu, P. Gong, *Molecules* **11**, 574 (2006)
- J. Sinkkonen, V. Ovcharenko, K.N. Zelenin, I.P. Bezhan, B.A. Chakchir, F. Al-Assar, K. Pihlaja, *Eur. J. Org. Chem.* **2002**, 2046 (2002)
- G. Hutchings, V. Polshettiwar, T. Asefa, *Nanocatalysis: Synthesis and Applications* (Wiley, New York, 2013)
- A. Amoozadeh, S. Golian, S. Rahmani, *RSC Adv.* **5**, 45974 (2015)
- M.B. Gawande, R. Luque, R. Zboril, *ChemCatChem* **6**, 3312 (2014)
- H. Moghanian, A. Mobinikhaledi, A. Blackman, E. Sarough-Farahani, *RSC Adv.* **4**, 28176 (2014)
- A. Mobinikhaledi, A.K. Amiri, *J. Chem. Sci.* **125**, 1055 (2013)
- M.A. Bodaghifard, M. Hamidinasab, N. Ahadi, *Curr. Org. Chem.* **22**, 234 (2018)
- D. Azarifar, O. Badalkhani, Y. Abbasi, M. Hasanabadi, *J. Iran. Chem. Soc.* **14**, 403 (2017)
- S. Joshi, M. Kumar, S. Chhoker, G. Srivastava, M. Jewariya, V. Singh, *J. Mol. Struct.* **1076**, 55 (2014)
- W.-F. Ma, Y. Zhang, L.-L. Li, L.-J. You, P. Zhang, Y.-T. Zhang, J.-M. Li, M. Yu, J. Guo, H.-J. Lu, *ACS Nano* **6**, 3179 (2012)
- M. Butterworth, L. Illum, S. Davis, *Colloids Surf. A Physicochem. Eng. Asp.* **179**, 93 (2001)
- S. Santra, R. Tapeç, N. Theodoropoulou, J. Dobson, A. Hebard, W. Tan, *Langmuir* **17**, 2900 (2001)
- Y. Lu, Y. Yin, B.T. Mayers, Y. Xia, *Nano Lett.* **2**, 183 (2002)
- A. Chaudhuri, M. Mandal, K. Mandal, *J. Alloys Compd.* **487**, 698 (2009)
- F. Nemat, M.M. Heravi, R.S. Rad, *Chin. J. Catal.* **33**, 1825 (2012)
- R. Sen, P. Jain, R. Patidar, S. Srivastava, R. Rana, N. Gupta, *Mater. Today* **2**, 3750 (2015)
- Z.-D. Li, H.-L. Wang, X.-N. Wei, X.-Y. Liu, Y.-F. Yang, W.-F. Jiang, *J. Alloys Compd.* **659**, 240 (2016)
- K. Nejati, R. Zabihi, *Chem. Cent. J.* **6**, 23 (2012)
- H.S. Kim, D. Kim, B.S. Kwak, G.B. Han, M.-H. Um, M. Kang, *Chem. Eng. J.* **243**, 272 (2014)
- K. Petcharoen, A. Sirivat, *Mater. Sci. Eng. B* **177**, 421 (2012)
- Z. Zhang, Y. Liu, G. Yao, G. Zu, Y. Hao, *Int. J. Appl. Ceram. Technol.* **10**, 142 (2013)
- F.M. Moghaddam, B.K. Foroushani, H.R. Rezvani, *RSC Adv.* **5**, 18092 (2015)
- M. Sayyafi, M. Seyyedhamzeh, H.R. Khavasi, A. Bazgir, *Tetrahedron* **64**, 2375 (2008)
- J.M. Khurana, D. Magoo, *Tetrahedron Lett.* **50**, 7300 (2009)
- S.R. Konda, B.R. Reguri, M. Kagg, *Der Pharma Chem.* **6**, 228 (2014)
- K. Mazaahir, C. Ritika, J. Anwar, *Chin. Sci. Bull.* **57**, 2273 (2012)
- R. Fazaeli, H. Aliyan, N. Fazaeli, *Open Catal. J.* **3**, 14 (2010)
- R.A. Kiasat, A. Mouradezadegun, J.S. Saghanezhad, *J. Serb. Chem. Soc.* **78**, 469 (2013)
- H.R. Shaterian, M. Ghashang, M. Feyzi, *Appl. Catal. A Gen.* **345**, 128 (2008)
- A.A. Amiri, S. Javanshir, Z. Dolatkah, M.G. Dekamin, *New J. Chem.* **39**, 9665 (2015)